NASA Technical Memorandum 85848

NASA-TM-85848

NASA-TM-85848 19840002012

Application of an Adaptive Blade Control Algorithm to a Gust Alleviation System

Shigeru Saito

September 1983

NASA

National Aeronautics and
Space Administration

15   1   1 RN/NASA-TM-85848
              DISPLAY 15/2/1
      84N10079*#   ISSUE 1   PAGE 12   CATEGORY 8   RPT#: NASA-TM-85848 A-9497
      NAS 1.15:85848   83/09/00   32 PAGES   UNCLASSIFIED DOCUMENT
UTTL: Application of an adaptive blade control algorithm to a gust alleviation
      system
AUTH: A/SAITO, S.
CORP: National Aeronautics and Space Administration. Ames Research Center,
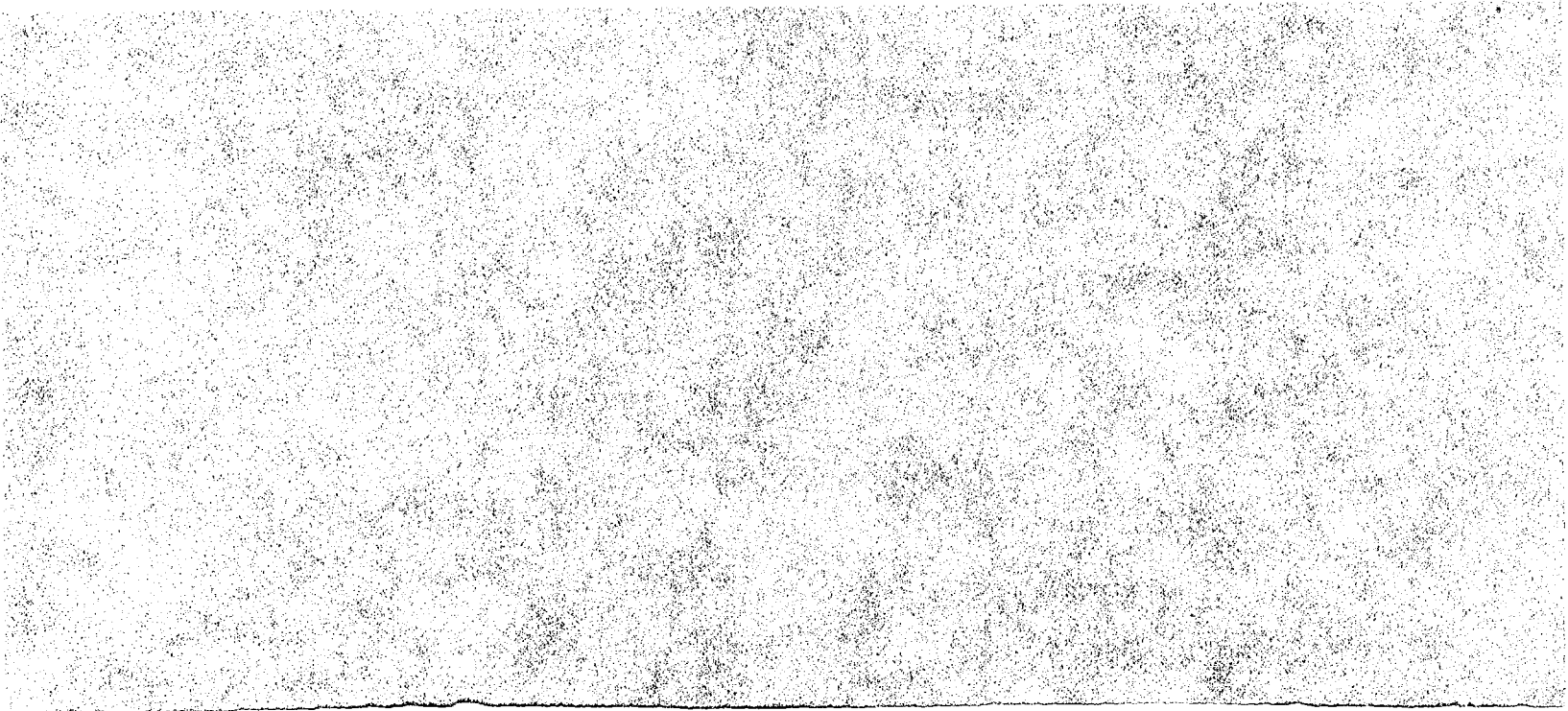   Moffett Field, Calif.   AVAIL.NTIS   SAP: HC A03/MF A01
MAJS: /*ADAPTIVE CONTROL/*ALGORITHMS/*GUST ALLEVIATORS/*HELICOPTERS/*ROTOR
      BLADES (TURBOMACHINERY)
MINS: / CONTROL THEORY/ HARMONIC ANALYSIS/ KALMAN FILTERS/ NUMERICAL ANALYSIS/
      PERTURBATION/ VIBRATION
ABA: Author
ABS: The feasibility of an adaptive control system designed to alleviate

Application of an Adaptive Blade Control Algorithm to a Gust Alleviation System

Shigeru Saito, NRC Associate, Ames Research Center, Moffett Field, California

NASA

National Aeronautics and
Space Administration

Ames Research Center
Moffett Field, California 94035

N84-10079 #

APPLICATION OF AN ADAPTIVE BLADE CONTROL ALGORITHM
TO A GUST ALLEVIATION SYSTEM

Shigeru Saito*

NASA Ames Research Center
Moffett Field, California 94035, U.S.A.

Abstract

The feasibility of an adaptive control system designed to alleviate helicopter gust-induced vibration has been analytically investigated for an articulated rotor system. This control system is based on discrete optimal control theory, and is composed of a set of measurements (oscillatory hub forces and moments), an identification system using a Kalman filter, a control system based on the minimization of the quadratic performance function, and a simulation system of the helicopter rotor. The gust models are step and sinusoidal vertical gusts. Control inputs are selected at the gust frequency (ω_G), subharmonic frequency ($\omega_G - \Omega$), and superharmonic frequency ($\omega_G + \Omega$), and are superimposed on the basic collective and cyclic control inputs. The response to be reduced is selected to be that at the gust frequency because this is the dominant response compared with sub- and superharmonics. Numerical calculations show that the adaptive blade pitch control algorithm satisfactorily alleviates the hub gust response. Almost 100% reduction of the perturbation thrust response to a step gust and more than 50% reduction to a sinusoidal gust are achieved in the numerical simulations.

Nomenclature

a	lift slope
b	semichord, $c/2$
C_H, C_T, C_Y	horizontal, thrust, and side force coefficients
C_{MX}, C_{MY}, C_{MZ}	rolling, pitching, and yawing moment coefficients
c	chord length
E( )	expectation of ( )
F_X, F_Y, F_Z	hub forces
f_G	gust frequency, Hz
g	gust velocity vector

---

*NRC Associate.

I_β moment of inertia of a blade about flapping hinge

$$= \int_{r_\beta}^{R} (r - r_\beta)^2 m \; dr$$

M_X, M_Y, M_Z hub moments

M_β mass moment of blade $= \int_{r_\beta}^{R} r(r - r_\beta) m \; dr$

m   blade section mass

Q   variance of the process noise

r   variance of the measurement noise

r_β position of flapping hinge

t   time

u_G, v_G, w_G horizontal, lateral, and vertical components of gust velocity

v   measurement noise

w   gust amplitude, m/sec

z   system response measurements

Δ perturbation from a steady value, or small increment

μ advance ratio

Ω rotor rotational speed, rad/sec

ω_G gust angular velocity, rad/sec

Subscripts:

C   control, or cosine element

G   gust

n   n time-cycle

S   sine element

0   initial value, or amplitude, or uncontrolled value

Superscripts:

$(^-)$ trimmed value

$(^\cdot)$ d( )/dt

(^)   estimate of ( )

( )^T transpose of ( )

1. Introduction

Helicopters fly close to the ground where the motion of the atmosphere may be thought of as turbulent flow. To avoid structural vibrations and unfavorable dynamic characteristics in flying and riding qualities caused by gusty winds, it is necessary to analyze the gust response of a rotary wing aircraft and develop a scheme to alleviate such responses.

Studies of gust responses of a helicopter rotor were reported in Refs. [1]-[5]; only Refs. [3] and [5] dealt with rotor gust response experiments. Experimental data for vertical gusts show that the thrust response was more sensitive than other responses of the rotor. For the sinusoidal gust with frequency (ω_G), the thrust response characteristics have not only a (ω_G) component, but also ($\omega_G + n\Omega$) (n = ± 1, ± 2, . . .) components in the fluctuation. In this thrust response, the (ω_G) element of the oscillatory characteristics is dominant in the comparatively low gust frequency range ($\omega_G \ll \Omega$).

Attempts to alleviate the gust-induced vibration have been described in Refs. [6]-[10]. Among them, Briczinski and Cooper [6] have investigated the effect of a rotor/vehicle state feedback system on the handling qualities of a helicopter, specifically characteristics concerned with gust response. They found that the feedback scheme of the rotor tip-path-plane or body state was very useful as a means of gust suppression. Johnson [7] studied the performance of an optimal control system applied to proprotor/wing gust response. Significant and simultaneous reduction in the rotor and wing responses was achieved. Zwicke et al. [8] investigated the performance of an optimal sampled-data feedback system on the gust response. They also studied a suboptimal feedback system derived from the above control system; a significant reduction in the gust response using this suboptimal feedback system was achieved. Ham and Mckillip [9] developed an individual blade control (IBC) scheme for gust response alleviation. Saito et al. [10] also studied a simple feedback system to alleviate rotor gust response; in their control scheme, individual blade pitch angle control, based on scheduled feedback gains derived from analytical calculations, is used.

There has been great progress in active control vibration reduction techniques for helicopters (theoretically and experimentally) in the past decade (Refs. [11]-[15]). In these vibration reduction systems, control schemes known as multicyclic control (Ref. [11]) or higher harmonic control (Ref. [13]) have been applied to the reduction of inherent vibratory responses of a helicopter. Pitch inputs at harmonics of the rotor rotational speed are used. Typically the helicopter is represented by a linear, quasi-static frequency domain model. The relationship between control inputs and outputs (which can include vibrations, loads, and rotor performance parameters) are modeled by a transfer function matrix. Theoretical

and experimental results show that the vibratory level of a helicopter
can be significantly reduced by using controllers in which the trans-
fer function matrix is updated by a Kalman filtering scheme. These
vibration reduction systems are reviewed in detail in Ref. [15].

In this paper, the feasibility of an adaptive control system
designed to alleviate gust-induced vibration has been analytically
investigated. This control system is based on a discrete optimal
control theory, and is composed of a set of measurements (oscil-
latory hub forces and moments), an identification system using a
Kalman filter, a control system based on the quadratic performance
function, and a simulation system of the helicopter rotor. The
gust models are step and sinusoidal vertical gusts. The local
momentum theory (LMT) (Ref. [16]) is used to calculate time-wise
vibratory airloads and moments at the hub position of the rotor. An
H-34 rotor with four articulated blades is used. The blades have
full flap, lead-lag and torsion elastic deflection. Fuselage motion
is not considered.

2. Adaptive Blade Pitch Control

An adaptive blade pitch control designed to alleviate gust-
induced vibration is analytically investigated. For the gust response
of a helicopter, additional vibratory responses, such as gust harmonic
(ω_G), subharmonic ($\omega_G - \Omega$), and superharmonic ($\omega_G + \Omega$), etc., appear
in the response. Gust harmonic response is dominant in the compara-
tively low gust frequency range (Refs. [3], [5]). Hence, this
response is selected as the response to be reduced. In this study,
the helicopter's gust response is characterized by time-dependent hub
forces and moments.

Helicopter Model

In this study, the helicopter is represented by a linear,
quasi-static frequency-domain model relating the output $\{z\}$ to the
input $\{\theta\}$. Here $\{z\}$ is an amplitude vector of the gust-induced
vibration harmonics in the nonrotating frame. The input $\{\theta\}$ is at
the gust frequency. It is assumed that the gust is sinusoidal, and
that the gust frequency is known a priori. When a rotor penetrates
into the gust, the hub oscillatory forces and moments can be consid-
ered to be composed of gust and control components:

$$\{z\} = \{z_G\} + \{z_C\} \tag{1}$$

Equation (1) can be rewritten by using the expression of the rotor
impedance $[T_G]$ and rotor transfer function $[T_C]$ as follows:

$$\{z_G\} = [T_G]\{g\}$$

$$\{z_C\} = [T_C]\{\theta\}$$

That is, Eq. (1) becomes

$$\{z\} = [T_G]\{g\} + [T_C]\{\theta\} \tag{2}$$

where

$$
\left.
\begin{aligned}
\{z\} &= (m \times 1) \text{ vector} \\
[T_G] &= (m \times 3) \text{ matrix} \\
\{g\} &= (3 \times 1) \text{ vector} \\
[T_C] &= (m \times n) \text{ matrix} \\
\{\theta\} &= (n \times 1) \text{ vector}
\end{aligned}
\right\} \tag{3}
$$

Once the hub response characteristics to a gust are determined, $[T_G]$ becomes a constant matrix. Therefore, we may denote the first term of Eq. (2) as $\{z_0\}$. Then Eq. (2) is

$$\{z\} = \{z_0\} + [T_C]\{\theta\} \tag{4}$$

This form resembles the global model formulation of helicopter vibration (Ref. [15]). The following "local model" can be also taken into account:

$$\{\Delta z\} = [T_C]\{\Delta\theta\} \tag{5}$$

where z means $z_n - z_{n-1}$ and $\Delta\theta$ means $\theta_n - \theta_{n-1}$.

Oscillatory hub forces and moments at the gust frequency in the nonrotating frame are chosen as the measurements $\{z\}$:

$$\{z\} = (F_{ZC}, F_{ZX}, F_{XC}, F_{XS}, M_{YC}, M_{YS}, F_{YC}, F_{YS}, M_{XC}, M_{XS}, M_{ZC}, M_{ZS}) \tag{6}$$

where the subscripts C and S denote the cosine and sine components of the hub reaction at the gust frequency ω_G. Control inputs are selected at the gust frequency (ω_G), subharmonic $(\omega_G - \Omega)$, and super-harmonic frequency $(\omega_G + \Omega)$ in the nonrotating frame as follows:

$$\Delta\theta = \theta_1 \cos(\omega_G t) + \theta_2 \sin(\omega_G t) + \theta_3 \cos(\omega_G - \Omega)t$$
$$+ \theta_4 \sin(\omega_G - \Omega)t + \theta_5 \cos(\omega_G + \Omega)t + \theta_6 \sin(\omega_G + \Omega)t \tag{7}$$

Hence the gust-control vector $\{\theta\}$ has the components

$$\{\theta\} = (\theta_1, \theta_2, \theta_3, \theta_4, \theta_5, \theta_6) \tag{8}$$

These control inputs are then superimposed on the blade trim pitch inputs.

Identification

Three cases are distinguished for the helicopter model, depending on the identification approach:

i. Identify $\{z_0\}$ only

ii. Identify $[T_C]$ only

iii. Identify $\{z_0\}$ and $[T_C]$

For the gust response, the uncontrolled response $\{z_0\}$ is generally time-variant; the matrix $[T_C]$ depends on the operating flight conditions. Hence it is necessary that a transfer function $[T_C]$ be identified simultaneously with the uncontrolled response $\{z_0\}$. Case iii is considered in this investigation. For the local model, it is necessary that the $[T_C]$ matrix be identified for each time-cycle. The Kalman filtering technique (Ref. [17]) is applied for identification. For the global model, Eq. (4) can be rearranged as follows:

$$z_n = z_0 + T_C\theta_n = [T_C, z](\theta_n, 1)$$

$$= T \cdot \theta_n \qquad (9)$$

where

$$T = m \times (n + 1) \quad \text{matrix}$$

$$\theta_n = (n + 1) \times 1 \quad \text{vector}$$

The subscript n denotes the time-step at $t = n \Delta t$. In this study, it is assumed that there is no noise in the measurement of θ_n. The identification algorithm can be derived by considering the jth measurement as

$$z_{jn} = \theta_n^T t_{jn} + v_{jn} \qquad (10)$$

where t_{jn} is the jth row of T and v_{jn} is measurement noise, which has zero mean $E(v_n) = 0$, variance $E(v_n v_m) = r_n\delta_{nm}$, and a Gaussian probability distribution. Here δ_{nm} is the Kronecker delta function and the subscript j will be omitted to simplify the notation. The variation of the parameters is modeled as a random process:

$$t_{n+1} = t_n + u_n \qquad (11)$$

where u_n is a random variable with zero mean $E(u_n) = 0$, variance $E(u_n u_m) = Q_n\delta_{nm}$, and a Gaussian probability distribution. The minimum error-variance estimate of t_n is then obtained from the Kalman filter (Ref. [17]).

$$\hat{t}_n = \hat{t}_{n-1} + k_n(z_n - \theta_n^T\hat{t}_{n-1}) \qquad (12)$$

where

$$M_n = P_{n-1} + Q_{n-1} \tag{13a}$$

$$P_n = M_n - M_n \theta_n \theta_n^T M_n / (r_n + \theta_n^T M_n \theta_n) \tag{13b}$$

$$k_n = M_n \theta_n / (r_n + \theta_n^T M_n \theta_n) \tag{13c}$$

Here M_n is the variance of the error in the estimate of t_n before the measurement, and P_n is the variance after the measurement. The parameter k_n is the Kalman gain vector. To simplify the calculation, it will be assumed that Q_n and r_n have the same time variation for all measurements, and that Q_n, r_n, and P_0 are proportional to the same function f_j: $r_{jn} = f_j r_n$; $Q_{jn} = f_j Q_n$; $P_{j0} = f_j P_0$. Then it follows that $P_{jn} = f_j P_n$ and $M_{jn} = f_j M_n$; and that the gain k_n is the same for all the measurements. With the same gains, the rows can be combined to form

$$\hat{T}_n = \hat{T}_{n-1} + (z_n - \hat{T}_{n-1}\theta_n)k_n^T \tag{14}$$

For the local model, Eq. (14) takes the following form:

$$\hat{T}_n = \hat{T}_{n-1} + [(z_n - z_{n-1}) - \hat{T}_{n-1}(\theta_n - \theta_{n-1})]k_n^T \tag{15}$$

where

$$M_n = P_{n-1} + Q_{n-1} \tag{16a}$$

$$P_n = M_n - M_n \Delta\theta_n \Delta\theta_n^T M_n / (r_n + \Delta\theta_n^T M_n \Delta\theta_n) \tag{16b}$$

$$k_n = M_n \Delta\theta_n / (r_n + \Delta\theta_n^T M_n \Delta\theta_n) \tag{16c}$$

$$\Delta\theta_n = \theta_n - \theta_{n-1} \tag{16d}$$

Controller

The control algorithm is based on the minimization of a performance index J that is a quadratic function of the input and output variables. The quadratic performance function used here is

$$J = z_n^T W_z z_n + \theta_n^T W_\theta \theta_n + \Delta\theta_n^T W_{\Delta\theta} \Delta\theta_n \tag{17}$$

where W_z, W_θ, and $W_{\Delta\theta}$ are weighting matrices, which are assumed to be diagonal, and all harmonics of a particular quantity have the same value. Then J is a weighted sum of the mean squares of the gust response and control. The matrix W_θ constrains the amplitude of the control and $W_{\Delta\theta}$ constrains the rate of change of the control.

For the deterministic controller, the control required to alleviate the helicopter vibration is given by substituting for z_n in the performance function J using the helicopter model and then solving for θ_n that minimizes J. For the global model (Eq. (4)) the solution can be obtained as follows:

$$\theta_n = Cz_0 + C_{\Delta\theta}\theta_{n-1} \tag{18}$$

where

$$C = -DT_C^T W_z \tag{19a}$$

$$C_{\Delta\theta} = DW_{\Delta\theta} \tag{19b}$$

$$D = (T_C^T W_z T_C + W_\theta + W_{\Delta\theta})^{-1} \tag{19c}$$

For the local model (Eq. (5)), the solution can be obtained as follows:

$$\theta_n = Cz_{n-1} + (C_{\Delta\theta} - CT_C)\theta_{n-1} \tag{20}$$

In this derivation the response z is assumed to be deterministic. When the parameter uncertainties are taken into account, the cautious controller can be obtained by using the expected value of the performance function:

$$J = E(z_n^T W_z z_n) + \theta_n^T W_\theta \theta_n + \Delta\theta_n^T W_{\Delta\theta}\, \Delta\theta_n$$

$$= E\left[\sum_j w_{zj} z_{jn}^2\right] + \theta_n^T W_\theta \theta_n + \Delta\theta_n^T W_{\Delta\theta}\, \Delta\theta_n \tag{21}$$

where it is assumed that W_z is diagonal, and θ_n is deterministic. For the case of the open-loop control (z_0 feedback), there follows

$$E\left[\sum_j w_{zj} z_{jn}^2\right] = E \sum_j [w_{zj}(z_{j0} + \theta_n^T t_{jn})^2]$$

$$= \sum_j w_{zj}(\hat{z}_{j0} + \theta_n^T t_{jn})^2$$

$$+ \sum_j w_{zj}(M_{zz} + 2\theta_n^T M_{tz} + \theta_n^T M_{tt}\theta_n) \tag{22}$$

where

$$M = \begin{bmatrix} M_{tt} & M_{tz} \\ M_{zt} & M_{zz} \end{bmatrix} \tag{23}$$

$$M_{tt} = (n \times m) \text{ matrix}$$

$$M_{tz} = M_{zt}^T = (n \times 1) \text{ vector}$$

$$M_{zz} = \text{scalar}$$

So the performance function becomes

$$J = z_n^T W_z z_n + \theta_n^T W_\theta \theta_n + (\theta_n^T, 1)\left(\sum_j w_{zj} M_{jn}\right)\binom{\theta_n}{1} + \Delta\theta_n^T W_{\Delta\theta} \Delta\theta_n \qquad (24)$$

The solution for the control that minimizes J is then

$$\theta_n = C z_0 + C_{\Delta\theta}\theta_{n-1} + C_0 \qquad (25)$$

The gain matrices C and $C_{\Delta\theta}$ are the same as for the deterministic controller using the identified values of the parameters and with W_θ replaced by

$$W_\theta + \left[\sum_j w_{zj}(M_{tt})_{jn}\right] \qquad (26)$$

The new constant term is

$$C_0 = -D\left[\sum_j w_{zj}(M_{tz})_{jn}\right] \qquad (27)$$

Similarly, for the case of the closed-loop control (z_{n-1} feedback), the performance function is

$$J = z_n^T W_z z_n + \theta_n^T W_\theta \theta_n + \Delta\theta_n^T\left(W_{\Delta\theta} + \sum_j w_{zj} M_{jn}\right)\Delta\theta_n \qquad (28)$$

The solution is identical to that for the deterministic controller using the identified values of the parameters and with $W_{\Delta\theta}$ replaced by

$$W_{\Delta\theta} + \sum_j w_{zj} M_{jn} \qquad (29)$$

Gust Model

In the past, studies dealing with gust-suppression systems have used gust models such as the von Kármán model, Dryden model, and step, sinusoidal, and sine-squares model, etc. These models have some advantages as well as disadvantages. The von Kármán and the Dryden models are expressions derived from statistical techniques in the frequency domain. These expressions are close to the natural turbulent flows in the sense of the statistics; however, they are not able to show the individual flow pattern of turbulence in the time domain. Therefore, they are not suitable for the time-wise numerical calculations. On the other hand, the step and sinusoidal gust models are very simple yet different from true gust shapes. These expressions are easy to handle in numerical calculations. In this study, the following gust representation is assumed:
$\{g\} = (u_G, v_G, w_G)^T = (u_{G0}, v_{G0}, w_{G0})^T \exp(i\omega_G t)$. Here u_{G0}, v_{G0}, and w_{G0} are horizontal, lateral, and vertical gust amplitudes, respectively. For the step gust, $\omega_G = 0$. For this study, the rotor

is assumed to have the blades at 0°, 90°, 180°, and 270° when the sinusoidal gust is initially encountered by the rotor (the gust velocity field is convected past the rotor by the helicopter forward speed).

Numerical Calculations

Numerical calculations have been performed to investigate this adaptive blade control algorithm. Blade properties and the rotor operating conditions are shown in Tables 1 and 2, respectively. The gust shape is schematically depicted in Fig. 1. The hub forces (F_X, F_Y, F_Z) and the hub moments (M_X, M_Y, M_Z) in the nonrotating frame are shown in Fig. 2. The initial estimate of the transfer function T_C is obtained by using a harmonic method program (Ref. [18]). Tables 3 and 4 show the transfer function of the rotor for $f_G = 2.0$ Hz and $f_G = 0.0$ Hz (step gust), respectively. For the step gust, gust frequency is assumed to be zero and the control inputs $\Delta\theta$ and the outputs z are assumed as follows:

$$\Delta\theta = \theta_1' + \theta_2' \cos \psi + \theta_3' \sin \psi$$

$$\{z\} = (\Delta F_{Z_0}, \Delta F_{X_0}, \Delta M_{Y_0}, \Delta F_{Y_0}, \Delta M_{X_0}, \Delta M_{Z_0})$$

(30)

where the subscript 0 denotes the mean value. The transfer function T_C obtained by the harmonic method is regarded as the initial estimation in the adaptive blade pitch control. In the controller, T_C is updated by the Kalman filter at every time-cycle. In this calculation, it is assumed that there is no noise in the $\Delta\theta$ measurement. Measurements z were contaminated by random measurement noise. Several sets of noise-to-signal ratios were studied before these calculations. A noise-to-signal ratio of 0.05 was used. The initial values of P_0 and Q_0 used in Eq. (19) were $P_0 = (9.8 \times 10^4)$ N (or N-m), $Q_0 = (9.8 \times 10^2)$ N (or N-m). The variance of the measurement noise, r, is assumed to be 9.8 N (or N-m). To keep the noise-to-signal ratio approximately constant, the following relationship is taken into account (see Ref. [8]): $r_{n+1} = r_n(J_{n+1}/J_n)$, $r_{min} < r_n < r_{max}$, where J_n is the quadratic performance function at the nth time-cycle. The weighting matrices of the quadratic performance function are $W_z = [1.0 \times 10^{-4}]$, $W_\theta = [0.0]$, $W_{\Delta\theta} = [1.0 \times 10^4]$.

Figure 3 is a schematic of the regulators used in this study: (a) adaptive open-loop and (b) adaptive closed-loop. In this gust alleviation system, the gust frequency is specified. Therefore, each time-cycle that updates the parameters must vary depending on the gust frequency. In most calculations, a 2.0 Hz gust frequency is used. This frequency is more than half of the rotor rotational speed, and somewhat larger than the typical mean atmospheric turbulence (usually below 1.0 Hz). An updated parameter estimate is performed every four revolutions of the rotor. During that time, the measurements z are discretely sampled. Since the measurements z are data in the time domain, they must be converted from time domain to frequency domain using the fast Fourier transform (FFT) (Ref. [19]). In the FFT, the resolution of the data in the frequency domain depends on the sampling time Δt (Shannon's theorem); in this calculation

$\Omega \Delta t = 10°$. Therefore, when the gust frequency f_G falls between two points (that is, $n \Delta f < f_G < (n + 1)\Delta f$, n = integer, Δf = frequency step), it is impossible to calculate the correct values by the FFT. In this analysis, correct values are approximated knowing the specified gust frequency f_G and using a cubic spline interpolation method. Furthermore, it is necessary to consider the calculation time of the optimal control, which determines the optimal control for the next time-cycle using the output data from the FFT. One time-cycle is 8π rad (see Fig. 4). The sampling interval is $(128/144)(8\pi)$ rad. Data are sampled at every 10° (144 samples in four revolutions); 128 is used in FFT sense power of 2 more efficient. Consequently the calculation time is assumed to be $(16/144)(8\pi)$ rad. As a result, there is a phase shift in the measured response at the beginning of the next time-cycle relative to the phase at the end of the previous sampling interval. This phase shift is accounted for in implementing the control. A global helicopter model is used. For the open-loop controller, both z_0 and T_C are updated by the Kalman filter. Only T_C is updated for the closed-loop controller.

Figures 5a to 5h show the hub gust responses with active blade pitch control for a vertical gust (f_G = 2.0 Hz). The control law is deterministic, and the global helicopter model was used. Two inputs (θ_1 and θ_2) and two outputs (cosine and sine elements of the thrust response) are considered. The thrust response (Fig. 5b) gradually decreases, but the modulated yawing moment response (Fig. 5g) is not minimized. The other responses (F_X, F_Y, M_X, M_Y) do not show any influence of the controller. Here the aim of the controller is to reduce only the thrust fluctuation caused by the gust; it does not reduce the other responses.

In Figures 6a to 6h, the hub responses are shown with active blade pitch control, again for the vertical gust. For these results the six control inputs (θ_1 to θ_6) are used to alleviate all 12 oscillatory hub responses. Measurements z involve the hub forces (F_X, F_Y, F_Z) and the hub moments (M_X, M_Y, M_Z). Compared with Fig. 5, the reduction of the thrust response is significant (from 50% to 80%). It is observed that the fluctuation of the thrust does not reduce uniformly. This phenomenon can be explained as follows. The control inputs generated by the controller depend on the measurements. When the hub responses are decreased by means of the controller, the optimal control inputs necessarily become smaller. At some point, apparently, the optimal control inputs become ineffective in generating rotor hub response. At the same time, the uncertainty of the identified parameters may increase because of measurement noise. In the yawing moment response (Fig. 6g) the convergence characteristics are improved relative to the two control input cases (see Fig. 5g). The amplitude of the fluctuation is somewhat less than the uncontrolled case. Similar to the thrust response, the response sometimes diverges and converges. This is due to the changes of the induced drag directly related to the thrust. Contrary to expectations, the responses (F_X, F_Y, M_X, M_Y) show a slight continuous increase in magnitude. In the pitch angle change of the reference blade (Fig. 6h), the change in the blade pitch with the gust frequency can be observed.

Figure 7 shows the time histories of the mean square thrust response. The solid line denotes the response without control. The dashed line corresponds to Fig. 5 (2 inputs and 2 outputs) and the broken line corresponds to Fig. 6 (6 inputs and 12 outputs). As explained before, the parameters are updated at every four revolutions. During one time-cycle, the control inputs are kept constant. The response for the case of thrust control only is at first constant, and then gradually decreases. The response is reduced by almost 50% after 30 revolutions (five time-cycles). The response for the case of complete hub response control decreases to a much lower value, although not continuously. A 50% to 80% reduction of the thrust response is attained for the case of complete hub response control. From these results, it is found that the measurements z should include not only the thrust response but also the other hub responses.

Figures 8a to 8h show the hub gust responses for a vertical step gust. In this case, the adaptive closed-loop controller is used. The measurements z involve only the longitudinal response of the rotor; that is, the horizontal force (F_X), the thrust (F_Z) and the pitching moment (M_Y). The control inputs have three elements (θ_1', θ_2', θ_3') according to Eq. (30). All parameters (z_0 and T_C) are updated at every rotor revolution by the Kalman filter. Significant reduction (nearly 100%) in the thrust response (Fig. 8b) is achieved by the controller. However, compared with the uncontrolled case, the horizontal and side force responses and the rolling and pitching moment responses transfer to slightly different steady state conditions. In the yawing moment response (Fig. 8g), there is a significant change in the steady state condition. This phenomenon comes from the strong effect of the controller on the gust alleviation system. The controller generates the optimal control inputs in order to reduce the fluctuation from the steady value. If these control inputs are significant values relative to the baseline trim pitch inputs, a new trim condition could result. Referring to Fig. 8h, the maximum change of the pitch angle is about 2°. The cyclic pitch angle for the trim condition is less than 2°. Therefore, the pitch angle change by the controller has an effect on the rotor trim condition. The flight trim condition changes and transfers to the new steady state condition.

In Fig. 9, the sensitivity of the adaptive closed-loop controller performance to the transfer function is investigated for the step gust. Arbitrary small initial values for the transfer function are used in this calculation. Again, only longitudinal hub responses are included in the plant model. Compared with Fig. 8, the thrust fluctuation (Fig. 9b) decreases very slowly. The other responses, except yawing moment, remain at the same trim condition. In the case of the yawing moment (Fig. 9g), the convergence to a new steady state can be seen after showing a significant transient. This phenomenon is due to the induced drag, as mentioned before. From these results, it can be concluded that the performance of the controller depends on the initial estimate of the rotor transfer function. If a more accurate transfer function is used, quick convergence of the responses can be obtained. The transfer function derived by the harmonic method provides a reasonable initial estimate.

Figures 10a to 10h show the hub responses for the vertical step gust with the adaptive open-loop controller. For these results, the measurements z involve all six responses of the rotor. All elements of T_C are updated at every rotor revolution. The magnitudes of the controller inputs are constrained by a prescribed maximum value, $\Delta\theta_{max} = 2.0°$. For the thrust response (Fig. 10b), the deviation from the steady value of the thrust only gradually decreases after responding to the step gust. The other hub forces together with the rolling and pitching moment remain steady. The yawing response deviates slowly from the steady value because of the thrust response. Compared with the case of Fig. 8, the pitch angle change is very slow and small. For the open-loop controller, the optimal control inputs depend on the uncontrolled response z_0. If the z_0 are small, then the optimal control inputs may be small. For this case, the optimal control inputs at the beginning stage of controller operation are less than $0.5°$.

In Fig. 11, the time histories of the quadratic performance function J are shown for the vertical step gust. A solid line denotes the time history of J for the uncontrolled case. The J with control are shown for both the adaptive closed-loop control (corresponding to Fig. 8) and the adaptive open-loop control (corresponding to Fig. 10). For the adaptive closed-loop controller, the J decreases rapidly after showing a sharp increase. The J for the adaptive open-loop controller decreases moderately after showing the same increase. Both control schemes demonstrate the effect the controller has on the reduction of the hub gust responses.

For the deterministic controller considered in this analysis, the uncertainty of the parameter identification has not been accounted for in the calculation of the optimal control inputs. The cautious properties can play an important role in helicopter vibration reduction schemes (Ref. [14]). In Figs. 12a to 12h, the hub gust responses with the cautious controller are shown for the vertical sinusoidal gust ($f_G = 2.0$ Hz). Referring to the results with the deterministic controller (Fig. 6), there is no significant difference between these controllers. The cautious controller involves the variance of the error in the estimate of the transfer function T before the measurement. The more uncertain the parameter estimates, the larger the variance of the error. In this case, the term concerned with the cautious properties

$$\sum_j w_{zj} (M_{tt})_{jn}$$

in Eq. (26) was about 1% of the term $T_C^T W_z T_C$ in Eq. (19c). Therefore, the cautious properties have little effect on the controller performance in this study.

Results from applying adaptive blade pitch control for a three-dimensional gust are shown in Figs. 13a to 13h. The three gust components have amplitudes $u_{G0} = 3.0$ m/sec, $v_{G0} = 2.0$ m/sec, and $w_{G0} = 1.8$ m/sec; all have frequency $f_G = 2.0$ Hz. A large reduction in the thrust response is observed. In general, all the hub responses

are similar to the case of a vertical gust only (Fig. 6). In this study it was observed that the rotor hub responses were most sensitive to the vertical gust component. For the three component gust, the controller's cautious properties are not considered because of their demonstrated minimal effect on controller performance for the one component gust case.

3. Conclusions

Feedback control systems to reduce the gust-induced vibration of a helicopter rotor have been studied by an adaptive blade pitch control. For the three gust components, the horizontal and lateral gust components have little influence on the hub gust response. However, the vertical component of gust has a significant influence. In studying the gust response the rotor thrust shows the most significant change compared with other hub responses. Hence, reducing the thrust response may be the only necessary aim of the gust alleviation system. In this study, the major, the subharmonic, and the superharmonic inputs in the nonrotating frame are considered in the controller. As the gust frequency increases, higher frequency terms of the gust response become large. To alleviate these high frequency terms in the vibratory response, the number of terms included in the control inputs increases, making the controller more complex. The gust frequency is prescribed at the initial stage of the calculations. Therefore, this type of regulator does not apply to random gust responses. From these theoretical results, the following conclusions can be drawn.

1. The performance of the controller depends on the initial estimate of the rotor transfer function. When the exact transfer function is used, the convergence of the responses can be achieved quickly. The transfer function derived by the harmonic method (Ref. [18]) gives a good estimate for initializing the controller.

2. In using the FFT to convert measurements from the time domain to the frequency domain, some approximation must be made because of the gust frequency. This may increase the uncertainty of the measurement. A more accurate frequency domain determination method is required.

3. Using a cautious controller to account for the uncertainty of the parameter identification has little influence on the improvement of the regulator performance.

4. For the case of a sinusoidal gust, the adaptive open-loop regulator is best suited for the gust alleviation system. Results show that a 50% to 80% reduction of the thrust response can be obtained. The regulator studied in this paper is shown to be applicable to a three dimensional gust.

5. For the step gust, the adaptive closed-loop regulator performs better than the adaptive open-loop regulator. The closed-loop regulator yields a rapid reduction of the gust-induced thrust response (almost 100%), even though it violates the trim condition. The open-loop regulator shows that convergence of the thrust response is slow.

References

1) J. M. Drees and K. W. Harvey: Helicopter Gust Response at High Forward Speed, Journal of Aircraft, Vol. 7, No. 3, May–June 1970.

2) D. J. Arcidiacono, R. R. Bergquist, and W. I. Alexander, Jr.: Helicopter Gust Response Characteristics Including Unsteady Aerodynamic Stall Effects, NASA SP-352, 1974.

3) M. Vasue: A Study of Gust Response for a Rotor-Propeller in Cruising Flight, NASA CR-137537, 1974.

4) M. Judd and S. J. Newman: An Analysis of Helicopter Rotor Response due to Gusts and Turbulence, Vertica, Vol. 1, No. 3, 1977.

5) A. Azuma and S. Saito: Study of Gust Response by Means of the Local Momentum Theory, presented at the 5th European Rotorcraft and Powered Lift Aircraft Forum, Sept. 4–7, 1979. Also, Journal of the American Helicopter Society, Vol. 27, No. 1, Jan. 1982.

6) S. J. Briczinski and D. E. Cooper: Flight Investigation of Rotor/ Vehicle State Feedback, NASA CR-132546, 1975.

7) W. Johnson: Optimal Control Alleviation of Tilting Proprotor Gust Response, Journal of Aircraft, Vol. 14, No. 3, Mar. 1977.

8) R. B. Taylor, P. E. Zwicke, P. Gold, and W. Miao: Analytical Design and Evaluation of an Active Control System for Helicopter Vibration Reduction and Gust Response Alleviation, NASA CR-152377, 1980.

9) N. D. Ham and R. M. Mckillip, Jr.: A Simple System for Helicopter Individual-Blade-Control and its Application to Gust Alleviation, presented at the 36th Annual National Forum of the American Helicopter Society, May 1980. Also presented at the 6th European Rotorcraft and Powered Lift Aircraft Forum, Sept. 16–19, 1980.

10) S. Saito, A. Azuma, and M. Nagao: Gust Response of Rotary Wing Aircraft and Its Alleviation, presented at the 6th European Rotorcraft and Powered Lift Aircraft Forum, Sept. 16–19, 1980. Also Vertica, Vol. 5, No. 2, 1981.

11) J. L. McCloud III: The Promise of Multicyclic Control for Helicopter Vibration Reduction, Vertica, Vol. 4, No. 1, 1980.

12) I. Chopra and J. L. McCloud III: Considerations of Open-Loop, Closed-Loop and Adaptive Multicyclic Control Systems, presented at the AHS Northeast Region National Specialists' Meeting on Helicopter Vibration Technology for the Jet Smooth Ride, Nov. 1981. Also, Journal of the American Helicopter Society, Vol. 28, No. 1, Jan. 1983.

13) J. Shaw: Higher Harmonic Blade Pitch Control: A System for Helicopter Vibration Reduction, Ph.D. thesis, Massachusetts Institute of Technology, Cambridge, Mass., May 1980.

14) J. A. Molusis, C. E. Hammond, and J. H. Cline: A Unified Approach to the Optimal Design of Adaptive and Gain Scheduled Controllers to Achieve Minimum Helicopter Rotor Vibration, presented at the 37th Annual National Forum of the American Helicopter Society, May 1981.

15) W. Johnson: Self-Tuning Regulators for Multicyclic Control of Helicopter Vibration, NASA TP-1996, 1982.

16) A. Azuma and K. Kawachi: Local Momentum Theory and Its Application to the Rotary Wing, Journal of Aircraft, Vol. 16, No. 1, Jan. 1979.

17) A. E. Bryson, Jr. and Yu.-Chi Ho: Applied Optimal Control: Optimization, Estimation and Control, Hemisphere Publishing Corporation, 1975.

18) S. Saito: A Study of Helicopter Gust Response Alleviation by Automatic Control, NASA TM-85848, Nov. 1983.

19) R. K. Otnes and L. Enochson: Applied Time Series Analysis, Vol. 1: Basic Techniques, John Wiley and Sons, 1978.

TABLE 1.- ROTOR CHARACTERISTICS

Rotor radius, R	8.53 m
Blade lift slope, a	5.73
Blade semichord, b	0.2185 m
Number of blades, N	4
Rotor rotational speed, Ω	23.67 rad/sec
Blade twist rate, θ_t	-8°
Position of flapping hinge, r_β	0.3 m
Blade cutoff, r_C	0.594 m
Blade c.g. position, r_{CG}	2.74 m
Position of lag damper, r_ζ	0.3 m
Lag damper coefficient, C_ζ	1000.0 N-m-sec/rad
Blade mass, m	106.4 kg
Moment of inertia of blade, I_β	1593.9 kg-m^2
Mass moment of blade, M_β	1659.1 kg-m^2
Lock number, γ	8.84
Wing section	NACA 0012
Gross weight, W	62259.4 N

TABLE 2.- OPERATING CONDITIONS

Advance ratio, μ	0.18
Collective pitch angle, θ_0	8.0°
Longitudinal pitch angle, θ_{1S}	-1.48°
Lateral pitch angle, θ_{1C}	0.695°
Inflow ratio, λ	0.0179

TABLE 3.- TRANSFER FUNCTION OF ROTOR FOR GUST FREQUENCY OF 2.0 Hz

$$[T_C] = \begin{bmatrix}
-25.52 & -576.5 & -192.6 & 22.40 & 81.50 & -11.92 \\
576.5 & -25.52 & 22.40 & -192.6 & 11.92 & 81.50 \\
9.831 & -59.62 & -211.6 & -44.92 & 50.86 & 53.35 \\
66.51 & 15.42 & 3.635 & -179.3 & -88.02 & 59.16 \\
34.46 & -112.7 & 2397 & -85.89 & 2561 & 91.49 \\
112.7 & 34.46 & 85.89 & 2397 & -91.49 & 2561 \\
-63.17 & 2.580 & -48.63 & 216.3 & -56.87 & 37.14 \\
-2.580 & -63.17 & -216.3 & -48.63 & -37.15 & -56.87 \\
-1185 & 4.166 & 96.97 & 2508 & 87.10 & -2618 \\
-4.166 & -1185 & -2508 & 96.97 & 2618 & 87.10 \\
969.5 & 77.35 & -10.06 & -293.7 & 4.302 & 202.5 \\
-77.35 & 969.5 & 293.7 & -10.06 & -202.6 & 4.305
\end{bmatrix} \times 10^2$$

TABLE 4.- TRANSFER FUNCTION OF ROTOR
FOR STEP GUST

$$[T_C] = \begin{bmatrix}
0.996 & 8.545 & 2.984 \\
-0.496 & 8.004 & 2.077 \\
1.849 & 1.872 & 0.635 \\
68.42 & 252.3 & 95.31 \\
-16.62 & 289.0 & 81.92 \\
8.599 & 17.79 & 5.652
\end{bmatrix} \times 10^3$$
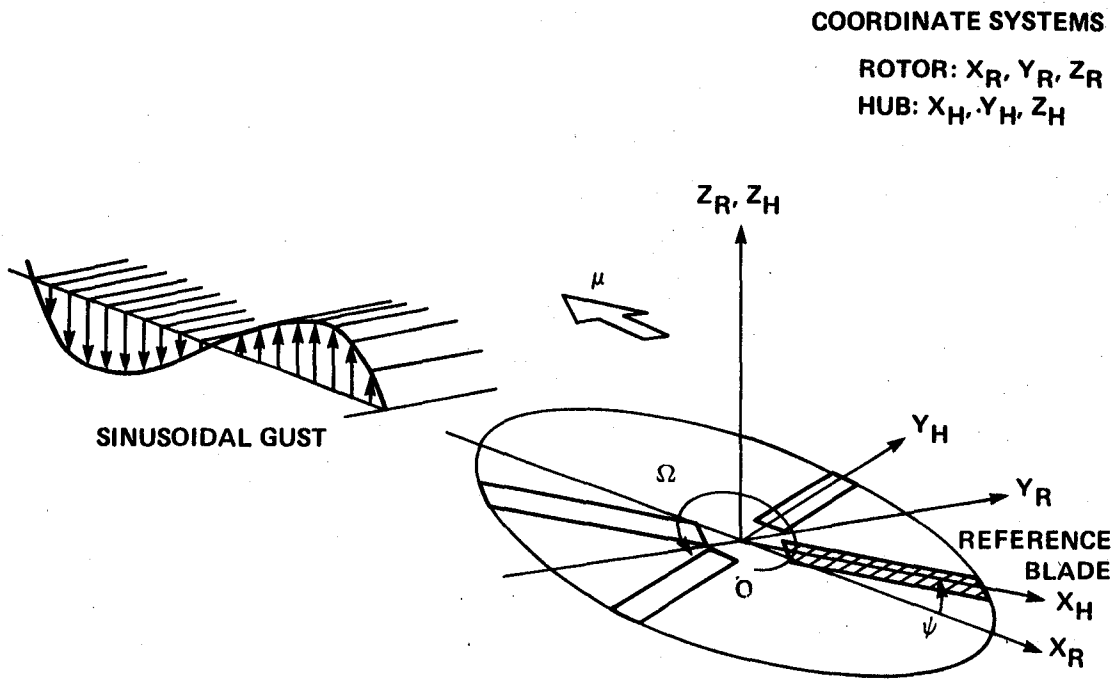
Fig. 1. Gust shape and coordinate systems.
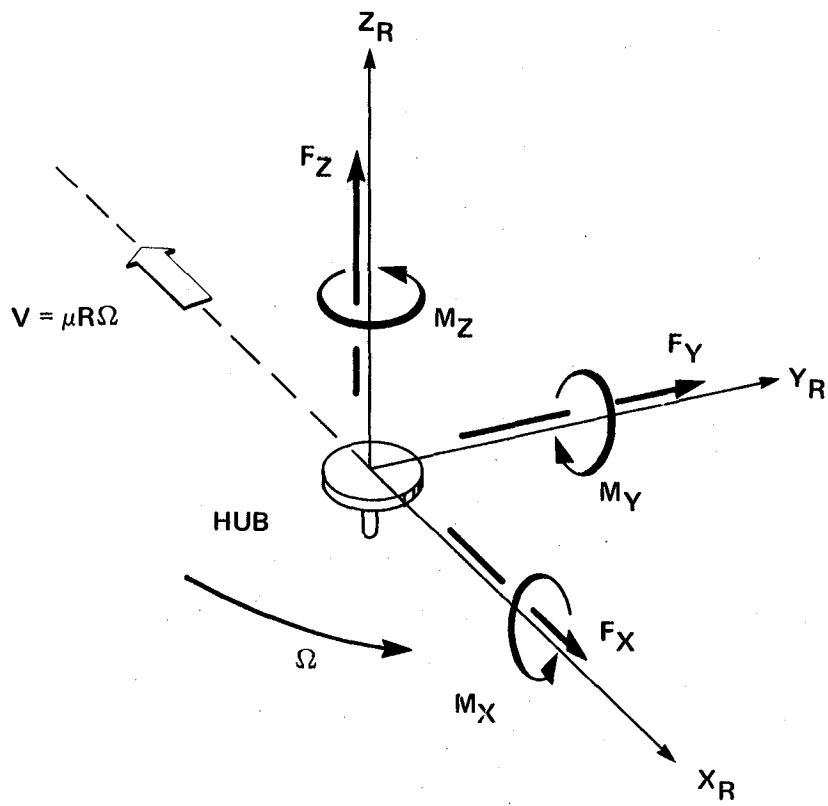
Fig. 2. Hub forces and moments.
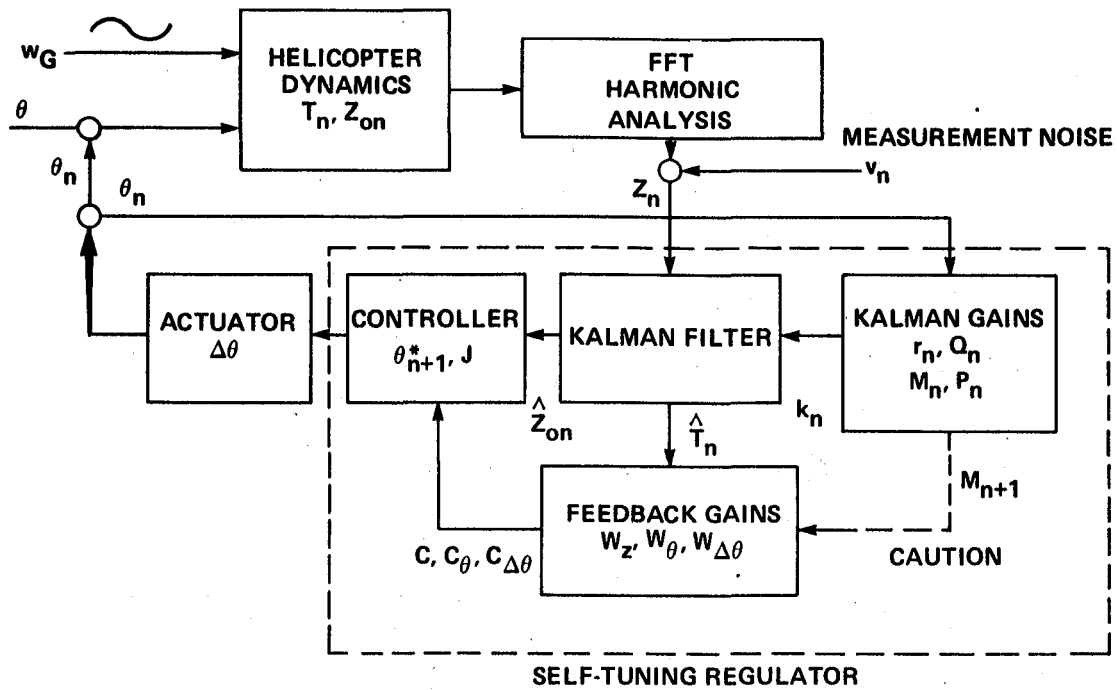
(a) Open-loop regulator.
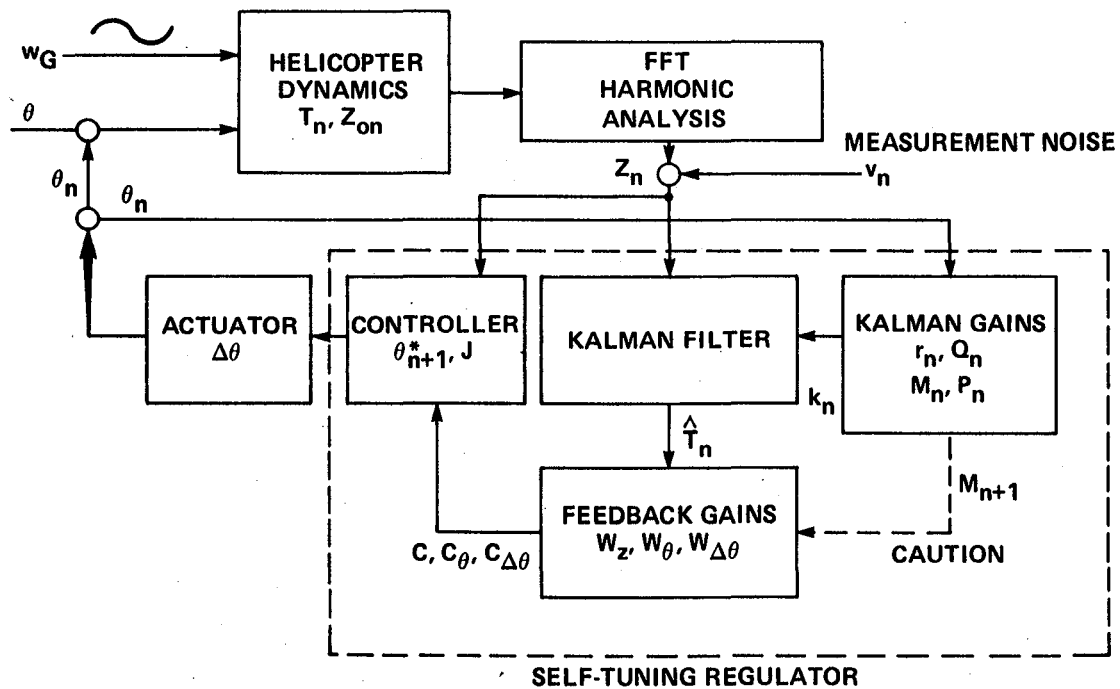
(b) Closed-loop regulator.

Fig. 3. Adaptive regulators for gust alleviation.
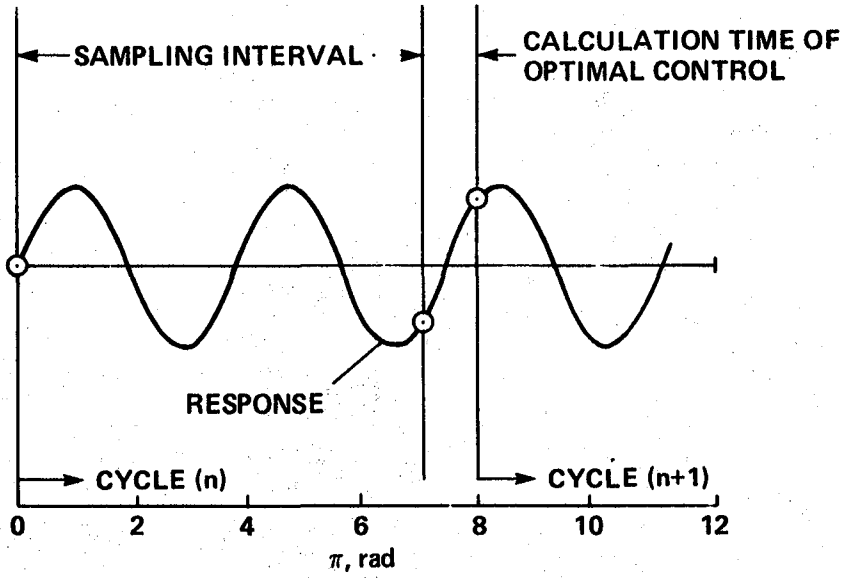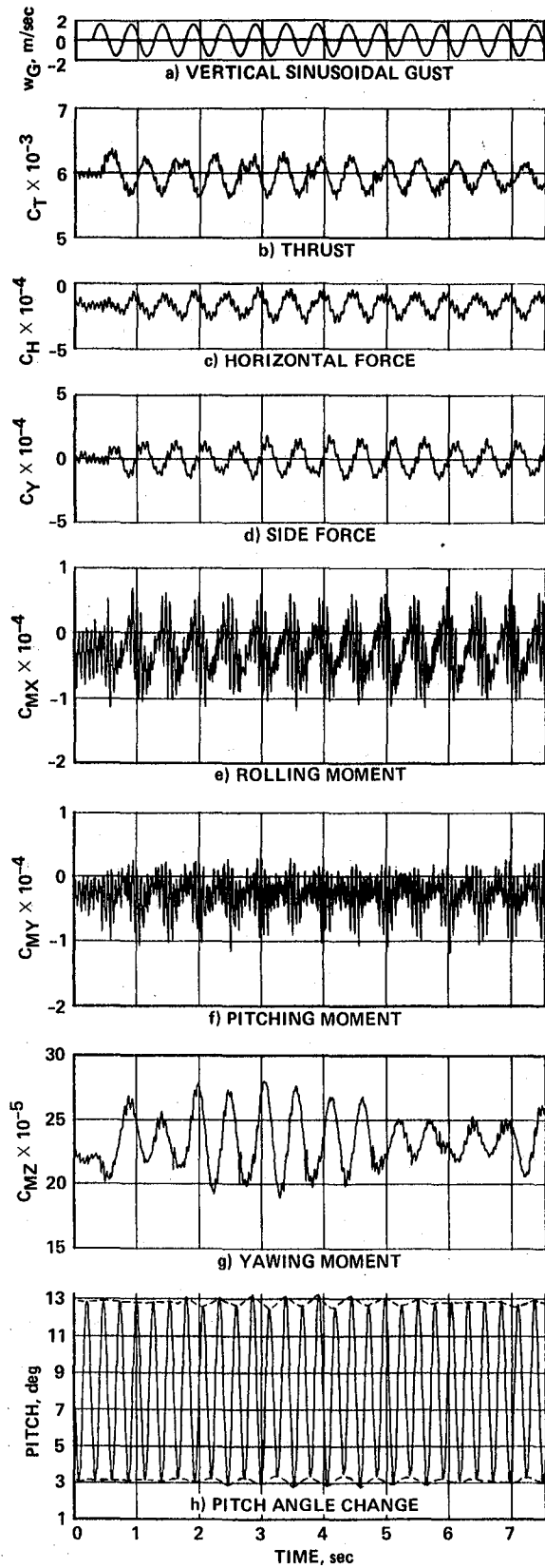
Fig. 4. Sequence of controller implementation.

Fig. 5. Time history of hub responses with adaptive open-loop blade pitch control for a vertical sinusoidal gust: $w_{G_0} = 1.8$ m/sec, $f_G = 2.0$ Hz.
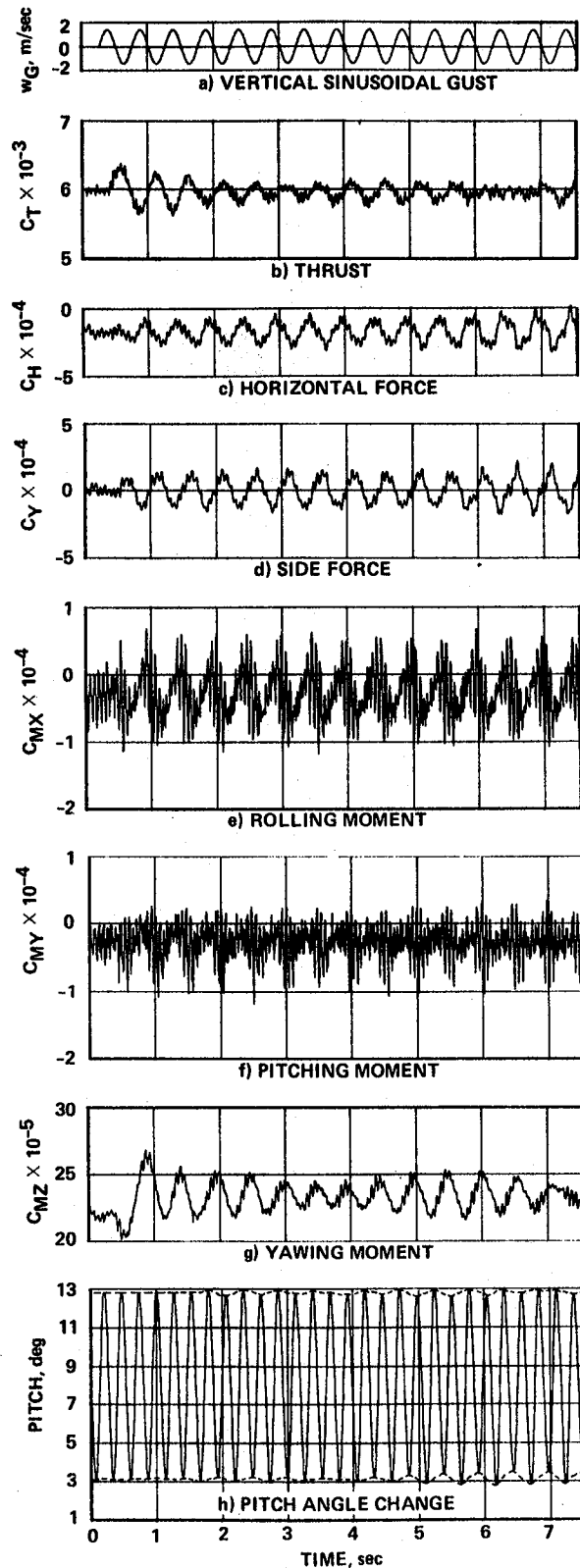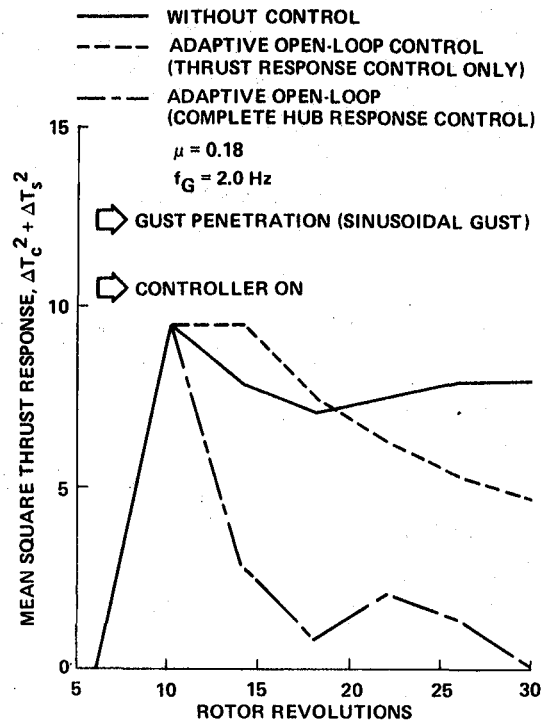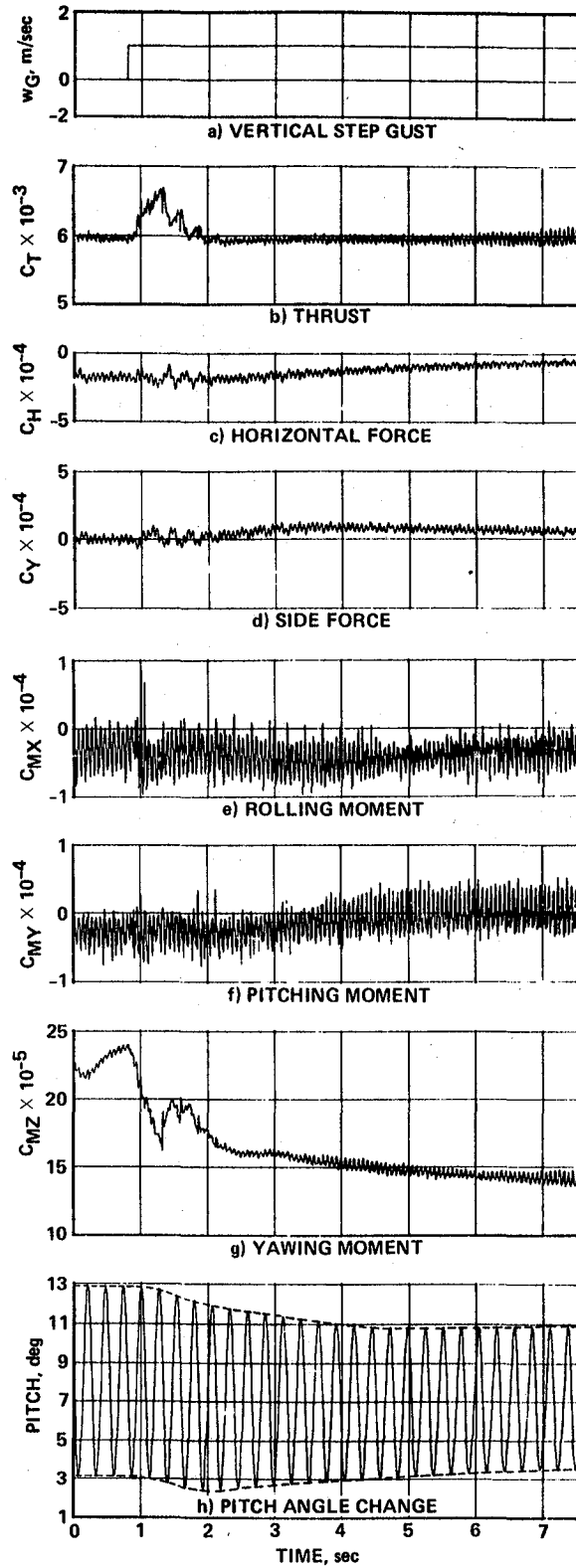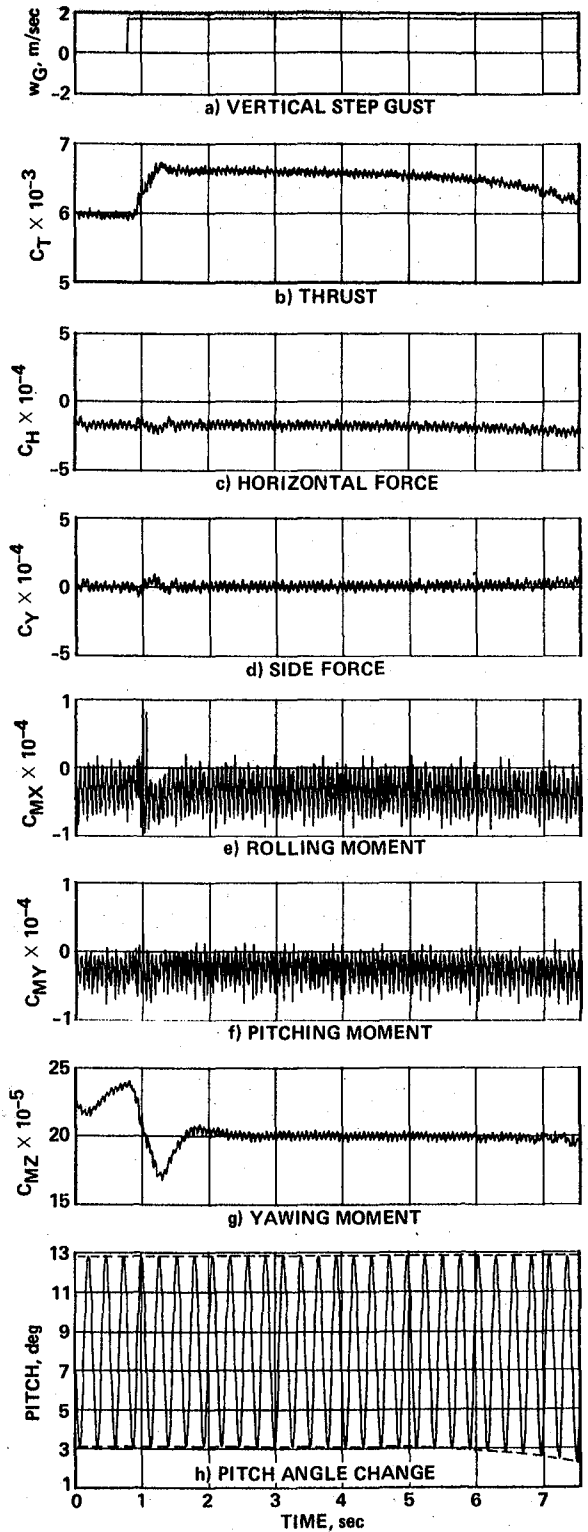
Fig. 6. Time history of hub responses with adaptive open-loop blade pitch control for a vertical sinusoidal gust: $w_{G0} = 1.8$ m/sec, $f_G = 2.0$ Hz.

Fig. 7. Time history of the mean square thrust.

Fig. 8. Time history of hub responses with adaptive closed-loop blade pitch control for a vertical step gust: $w_{G0} = 1.8$ m/sec.

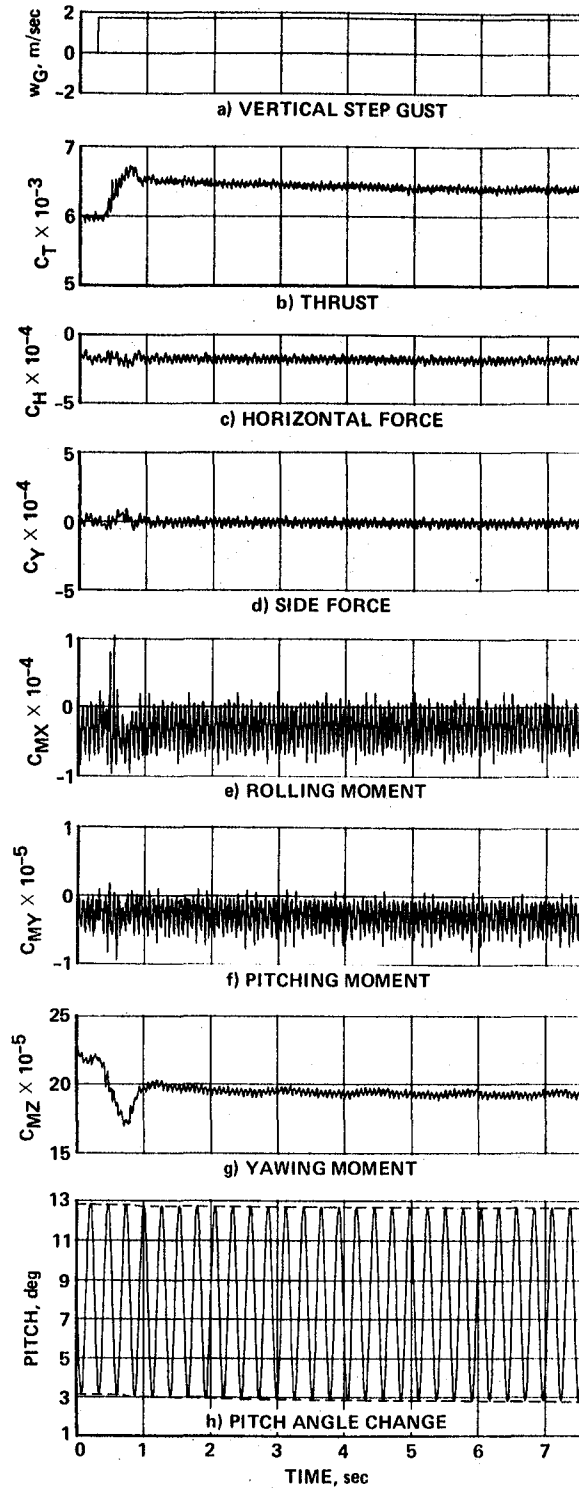Fig. 9. Time history of hub responses with adaptive closed-loop blade pitch control for a vertical step gust: $w_{G0} = 1.8$ m/sec.

Fig. 10. Time history of hub responses with adaptive open-loop blade pitch control for a vertical step gust: w_{G0} = 1.8 m/sec.
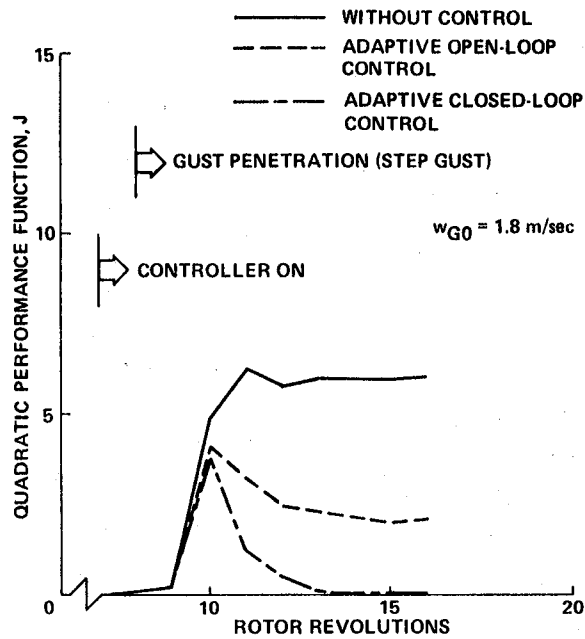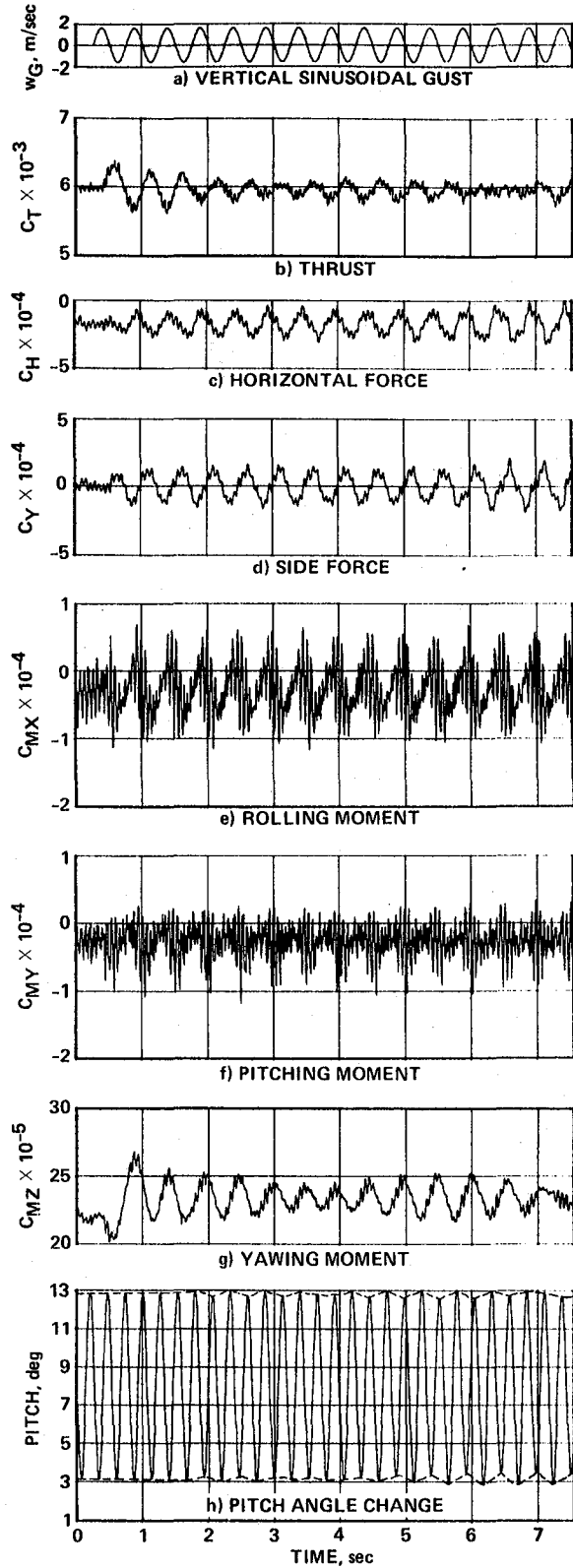
Fig. 11. Time history of quadratic performance function J.

Fig. 12. Time history of hub responses with adaptive open-loop blade pitch control with caution for a vertical sinusoidal gust: $w_{G0} = 1.8$ m/sec, $f_G = 2.0$ Hz.
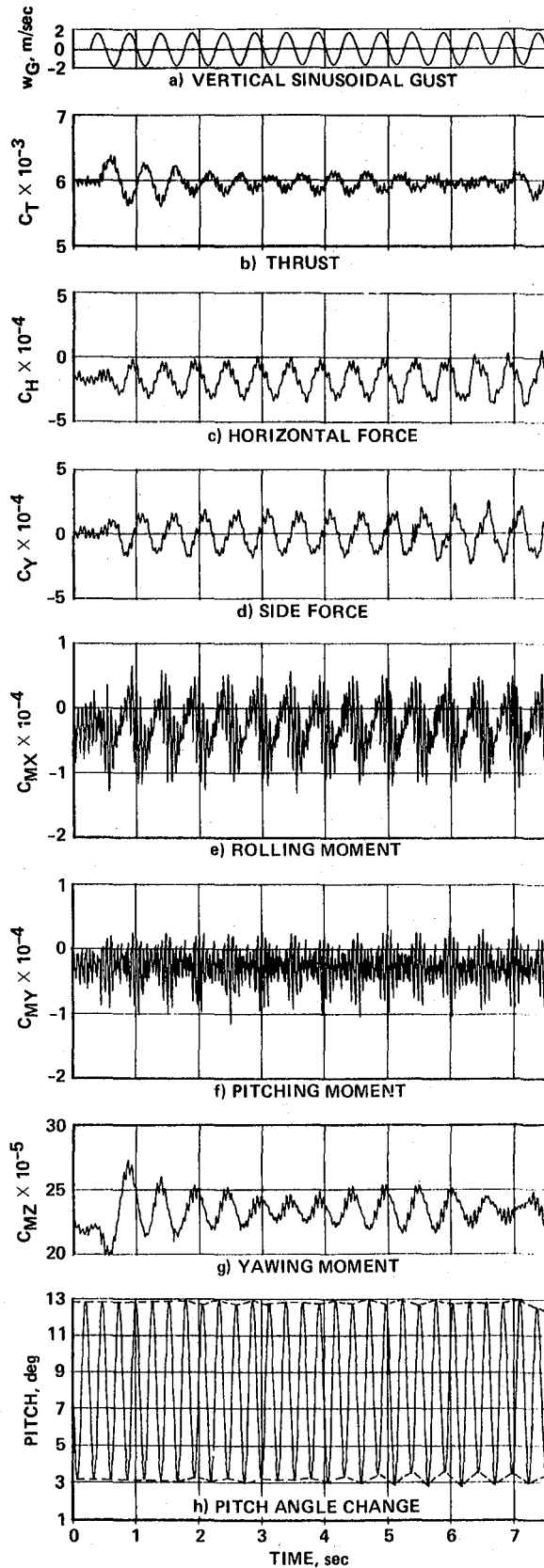
Fig. 13. Time history of hub responses with adaptive open-loop blade pitch control for three dimensional gust: $u_{G0} = 3.0$ m/sec, $v_{G0} = 2.0$ m/sec, $w_{G0} = 1.8$ m/sec, $f_G = 2.0$ Hz.

1. Report No. NASA TM 85848	2. Government Accession No.	3. Recipient's Catalog No.
4. Title and Subtitle APPLICATION OF AN ADAPTIVE BLADE CONTROL ALGORITHM TO A GUST ALLEVIATION SYSTEM		5. Report Date September 1983
		6. Performing Organization Code
7. Author(s) Shigeru Saito*		8. Performing Organization Report No. A-9497
9. Performing Organization Name and Address NASA Ames Research Center Moffett Field, California 94035		10. Work Unit No. T-5484A
		11. Contract or Grant No.
12. Sponsoring Agency Name and Address National Aeronautics and Space Administration Washington, D.C. 20546		13. Type of Report and Period Covered Technical Memorandum
		14. Sponsoring Agency Code 505-42-11

16. Abstract

    The feasibility of an adaptive control system designed to alleviate helicopter gust-induced vibration has been analytically investigated for an articulated rotor system. This control system is based on discrete optimal control theory, and is composed of a set of measurements (oscillatory hub forces and moments), an identification system using a Kalman filter, a control system based on the minimization of the quadratic performance function, and a simulation system of the helicopter rotor. The gust models are step and sinusoidal vertical gusts. Control inputs are selected at the gust frequency (ω_G), subharmonic frequency ($\omega_G - \Omega$), and superharmonic frequency ($\omega_G + \Omega$), and are superimposed on the basic collective and cyclic control inputs. The response to be reduced is selected to be that at the gust frequency because this is the dominant response compared with sub- and super-harmonics. Numerical calculations show that the adaptive blade pitch control algorithm satisfactorily alleviates the hub gust response. Almost 100% reduction of the perturbation thrust response to a step gust and more than 50% reduction to a sinusoidal gust are achieved in the numerical simulations.

17. Key Words (Suggested by Author(s)) Adaptive blade control algorithm Gust alleviation system Vertical sinusoidal and step gust	18. Distribution Statement Unlimited Subject Category - 08		
19. Security Classif. (of this report) Unclassified	20. Security Classif. (of this page) Unclassified	21. No. of Pages 32	22. Price* A03